

## Article

# Effects of COVID-Induced Mobility Restrictions and Weather Conditions on Air Quality in Hungary

Adrienn Varga-Balogh , Ádám Leelőssy \* and Róbert Mészáros

Department of Meteorology, Eötvös Loránd University, H-1117 Budapest, Hungary; vargabaloghadrienn@gmail.com (A.V.-B.); mrobi@nimbus.elte.hu (R.M.)

\* Correspondence: adam.leelossy@ttk.elte.hu

**Abstract:** Similarly to other countries, the first wave of the COVID pandemic induced a collapse of mobility in Hungary during the spring of 2020. From the environmental perspective, the obtained road traffic reduction of 20–50% could be regarded as an undesired traffic regulation experiment. Air quality impacts within Hungary were evaluated based on data from 52 monitoring sites measuring concentrations of pollutants  $\text{NO}_x$ ,  $\text{O}_3$ , and  $\text{PM}_{10}$ . Air pollution during the lockdown was compared to the same period (February–June) in the reference years 2014–2019. The large spatial heterogeneity of the air quality response was explored. The emission reduction coincided with the extreme weather of 2020, characterized by unusually warm pre-lockdown February and spring drought. The anomalously low pre-lockdown air pollution was further reduced ( $\text{NO}_x$ ) or increased ( $\text{PM}_{10}$ ) during the restrictions. Compared to the previous years,  $\text{NO}_x$  concentrations during the curfew were found to differ between  $-4.1$  and  $+0.2$  standard deviations (median  $-1.55$  SD), or  $-45\%$  and  $+3\%$  (median  $-18\%$ ) among different monitoring locations. Ozone concentrations were unusually high due to both weather and chemical reasons (median  $+11\%$  or  $+0.8$  SD), while the  $\text{PM}_{10}$  response was modest and largely weather-driven (median  $+7\%$  or  $+0.4$  SD).

**Keywords:** urban air quality; traffic emission; Hungary; COVID;  $\text{PM}_{10}$ ;  $\text{NO}_x$



**Citation:** Varga-Balogh, A.; Leelőssy, Á.; Mészáros, R. Effects of COVID-Induced Mobility Restrictions and Weather Conditions on Air Quality in Hungary. *Atmosphere* **2021**, *12*, 561. <https://doi.org/10.3390/atmos12050561>

Academic Editors: Gunnar W. Schade, Nicole Mölders, Daniele Contini, Gabriele Curci, Francesca Costabile, Prashant Kumar and Chris G. Tzanis

Received: 23 March 2021

Accepted: 23 April 2021

Published: 27 April 2021

**Publisher's Note:** MDPI stays neutral with regard to jurisdictional claims in published maps and institutional affiliations.



**Copyright:** © 2021 by the authors. Licensee MDPI, Basel, Switzerland. This article is an open access article distributed under the terms and conditions of the Creative Commons Attribution (CC BY) license (<https://creativecommons.org/licenses/by/4.0/>).

## 1. Introduction

The global response to the COVID pandemic brought an undesired air pollution reduction experiment throughout the world. The scientific potential of this unfortunate environmental experiment has been exploited worldwide by intensive research on the COVID-air quality (COVID-AQ) response. Early reports of urban  $\text{NO}_x$  concentration reduction, reaching 40–50% compared to the previous years, have been published from the first COVID hotspots, such as Wuhan [1], Milan [2], and Madrid [3]. Meanwhile, a general increase in ozone levels has also become evident, attributable to the “weekend effect”, or, in this case, the more pronounced “lockdown effect” of  $\text{NO}_x$ – $\text{O}_3$  chemistry [4,5]. After the first wave of the pandemic, air pollution reduction has been reported from numerous locations worldwide [6–11], and air quality was soon identified as a mediating factor between mobility reduction and COVID cases [12–14]. However, systematic investigation of global measurements revealed that the air quality improvement was not necessarily observable for every location in their respective lockdown period, and, notably, the Central-Eastern European region suffered a major increase in  $\text{PM}_{2.5}$  concentrations during the lockdown [8]. Furthermore, a large-scale transport episode was demonstrated, causing adverse changes in air pollution in the lockdown period in Hubei, China [15]. Especially particulate matter (PM) concentrations showed a very heterogeneous global and regional response, ranging from a decrease of 40–60% [16] through near-stagnation [7,17–19] to 20–30% increase [20]. In general, China and India experienced major improvement in both  $\text{NO}_x$  and PM levels [16], while the European and American response was more modest and restricted to  $\text{NO}_x$  at most locations [4,6,7,10,18,20,21]. The lack of general PM reduction

in Europe was attributed to the larger contribution of non-traffic emissions, including seasonal agricultural activities, and also to weather impacts [21], while meteorology was judged to be only a secondary factor in China [9].

Three main approaches exist for the selection of the reference period: (a) the pre-lockdown period [3,7,8,16], (b) the lockdown period in the previous years [6,10,17,20], and (c) model estimates for the lockdown period [20–25]. Other efforts to overcome these issues include weather analogies [2,26], comparing changes in air quality to changes in boundary layer height [10], and time series breakpoint detection [18,25]. The optimal method for each case depends on the available data and models as well as the regional characteristics. This, on the other hand, challenges the comparison of different results and the synthesis of a global perspective.

This study aims to contribute to the exploration of the COVID-AQ response from the Hungarian perspective. Previous research [10] showed a decrease in NO<sub>x</sub> concentrations in the city area of the Hungarian capital city, Budapest, while PM levels were not considerably affected and ozone concentration slightly increased. This study explores the regional heterogeneity of the COVID-AQ response by using air quality data from urban, suburban, and rural monitoring sites in Hungary.

## 2. Background and Data

### 2.1. The Study Region

The basin formed by the Carpathian Mountains creates adverse conditions for air pollution, and stagnation episodes often occur, especially in the winter [27]. Concentration guidelines defined by the European Environmental Agency (EEA) are regularly exceeded for NO<sub>x</sub> and PM<sub>10</sub> [28], and Budapest was found to be among the most affected European cities by air pollution health risks [29]. In 2018, 34% of annual domestic NO<sub>x</sub> emissions were attributable to passenger cars, 6% to other transportation, and 26% to agriculture [28]. However, the contribution to primary PM<sub>2.5</sub> emissions is only 6% from transportation and 3% from agriculture, faded by the dominant residential emissions (82%). Furthermore, a study has shown that approximately  $\frac{3}{4}$  of annual PM air pollution in Hungary is of transboundary origin [30], although serious winter air pollution episodes are caused by local sources [31]. It must be noted that the seasonality of the presented ratios is significant. Residential heating emissions dominate the winter. Agricultural emissions peak in early spring (through nitrogen fertilizers and dust suspension from bare soils), as well as during the late autumn burnings.

### 2.2. Data and Method

Air pollution monitoring data was obtained from the Hungarian Air Quality Monitoring Network (OLM) for the period 2014–2020. Observations from 52 fixed monitoring sites were available, 12 of which were located in the capital city of Budapest (Figure 1). Daily mean concentrations of PM<sub>10</sub>, NO<sub>x</sub>, and O<sub>3</sub> were generally available for investigation. All gas analyzers and dust monitors used in the monitoring network are based on reference methods or standards. PM<sub>10</sub> is measured at each measuring site by Grimm EDM 180 (optical), or Environnement SA MP101M (beta attenuation), or Thermo Scientific FH62 C14 (beta attenuation) sensor. NO<sub>x</sub> measurements are carried out Thermo Scientific 42i, or Environnement SA AC32M, or Teledyne API T200 sensor, while O<sub>3</sub> is measured by Thermo Scientific 49i, or Environnement SA O3 42M, or Teledyne API T400 sensor at each site. Maintenance of all sensors is provided by the Air Quality Reference Centre of Hungarian Meteorological Service, which includes periodic calibrations in reference laboratory based on EU directives and Hungarian standards (for more details, see: <http://levegominoseg.hu>, accessed on 18 April 2021). The air quality monitoring network of OLM covers the majority of major Hungarian towns. Station IDs referred further in the text are shown in Figure 1, while their names and other characteristics are enlisted in Appendix A.

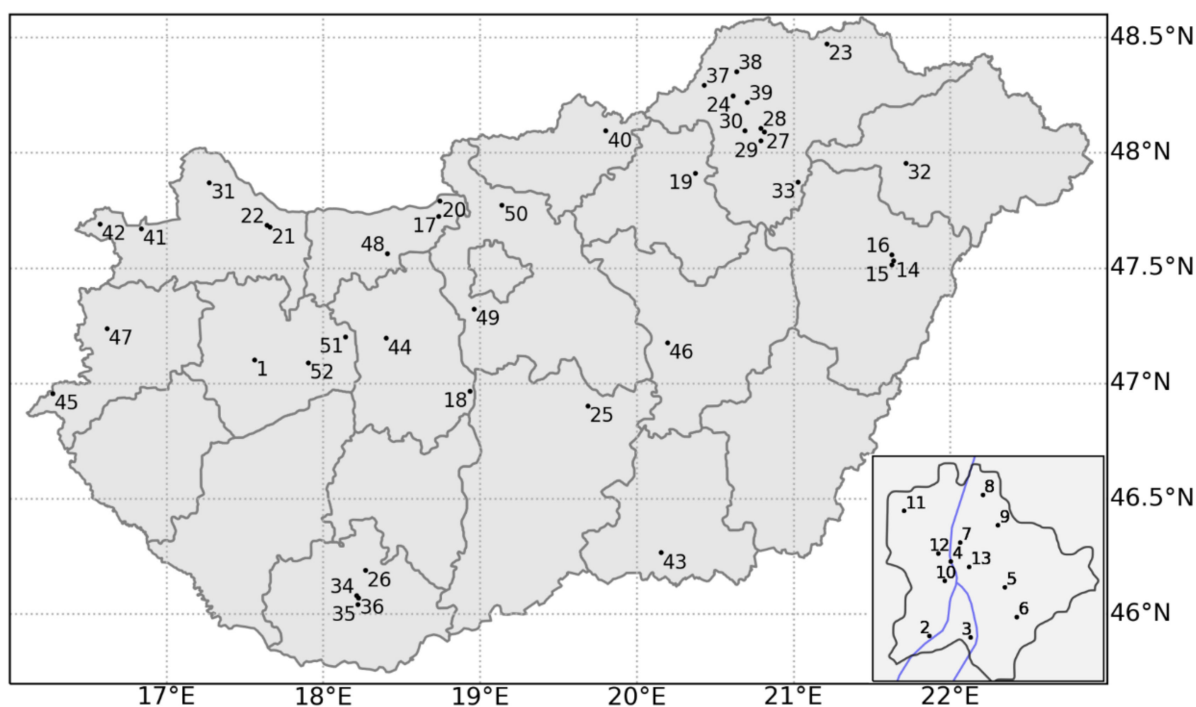


**Figure 1.** Air pollution monitoring sites in Hungary and the capital city Budapest (lower right). See detailed list in Appendix A.

Due to the strong seasonality of air pollution in Hungary, air pollutant concentrations in 2020 were compared to those obtained in the same period of 2014–2019. The difference between the mean concentration of 2020 and the respective means in previous years was expressed in terms of the  $z$  value, i.e., relative to the sample standard deviation of 2014–2019.

$$z = \frac{\mu_{2020} - \mu_{2014-2019}}{\sigma_{2014-2019}} \quad (1)$$

where  $\mu$  is the mean concentration for the respective period and  $\sigma$  is the sample standard deviation (SD) of the mean concentrations among the 6 previous years. If air pollutant concentrations of the same period over consecutive years were normally distributed,  $z = -1.96$  would mark a significant decrease in air pollution at a 95% level, compared to the previous years, while  $z = -0.67$  would sign the 50% significance level.

### 2.3. Traffic Reduction in the Study Period

Two periods were defined for the investigation: 12 March–16 June and 28 March–4 May, named “emergency” and “curfew”, respectively (Figure 2). A general estimate for countrywide traffic reduction can be obtained by the fuel consumption, reduced by 18–19% in April–June compared to the same quarter of 2019 (data from the Hungarian Petroleum Association). The Google Community Mobility Reports (<https://www.google.com/covid19/mobility/>, accessed on 18 April 2021) obtained a mean mobility reduction of 50% and 40% at transit stations in the curfew and emergency period, respectively. For more accurate fixed-point observations, camera-based traffic density monitoring data was obtained from the Budapest road network operator (Figure 2 and Table 1). The public emergency initiated a rapid collapse of mobility in mid-March and ended with a slow, gradual rearrangement during May and early June. The urban road traffic stabilized at 50–70% of pre-lockdown intensity for the curfew period (Figure 2 and Table 1). Dates marked in Figure 1: 4-March: first COVID case in Hungary; 12-March: public emergency, partial lockdown affecting schools, tourism, culture and administration, stay-at-home campaign; 28-March: general curfew restrictions; 4-April: lifting parking fees to unburden private car usage for essential

travels; 12-April: Easter holiday; 4-May: gradual reopening begins in Hungary; 16-May: gradual reopening begins in Budapest; 16-June: public emergency withdrawn.

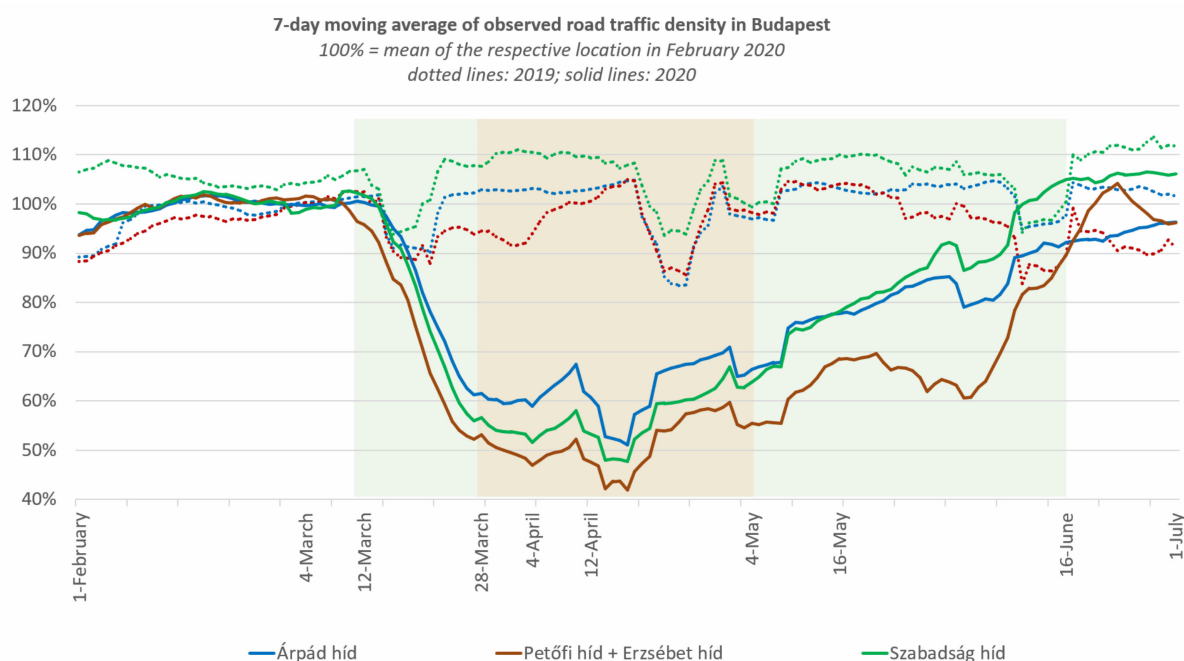


**Figure 2.** Seven-day moving average of observed road traffic density in Budapest at different cross-sections (dotted lines: 2019, solid lines: 2020). A total of 100% equals the mean traffic density of February 2020 (pre-lockdown) at the respective sites. Study periods are marked with colored boxes (green: “emergency” with partial lockdown; red: “curfew” with general mobility restrictions). Data from Budapest Public Roads Company (Budapest Közút).

**Table 1.** COVID-related traffic reduction at different road cross-sections of Budapest.

Period	Suburban (Árpád híd)	Urban (Erzsébet híd + Petőfi híd)	City (Szabadság híd)
Public emergency (12 March–16 June)	−26% <sup>1</sup> −26% <sup>2</sup>	−38% <sup>1</sup> −36% <sup>2</sup>	−27% <sup>1</sup> −30% <sup>2</sup>
Curfew restrictions (28 March–4 May)	−38% <sup>1</sup> −37% <sup>2</sup>	−49% <sup>1</sup> −48% <sup>2</sup>	−44% <sup>1</sup> −47% <sup>2</sup>
Lowest 7-day mean	−49% <sup>1,3</sup> −41% <sup>1,4</sup>	−58% <sup>1,3</sup> −53% <sup>1,4</sup>	−52% <sup>1,3</sup> −48% <sup>1,4</sup>

<sup>1</sup> related to the mean of the pre-lockdown period (February 2020). <sup>2</sup> related to the same period in 2019. <sup>3</sup> 11–17 April (the Easter holiday period with approx. 20% traffic reduction in a normal year). <sup>4</sup> 29 March–4 April (lowest 7-day mean traffic in 2020 excluding the Easter holiday). Data from Budapest Public Roads Company (Budapest Közút).

#### 2.4. Meteorological Conditions in the Study Period

The first wave of the pandemic coincided with a spring drought affecting the Carpathian Basin. The pre-lockdown in February 2020 was extremely warm with a monthly mean temperature of 5 °C (climatological mean 0.5 °C between 1981–2010). Freezing temperatures were caused by late March cold fronts (21 March, 30 March) transporting very dry air mass of polar origin. On 26 March, the easterly current transported dust to the southern part of Hungary from the deserted region near the Aral Sea [32]. Precipitation in April was limited to a few days and remained under 20 mm for most of the country or under 5 mm in the northwestern region (climatological mean 35–40 mm). No precipitation occurred in Hungary between 31 March and 11 April, almost exactly overlapping with the first two weeks of the curfew. In May, several cold fronts brought lower temperature

(monthly mean temperature 14 °C, climatological mean 16 °C) but caused only a small amount (20–50 mm) of precipitation. Meanwhile, precipitation during May in the central region of Budapest remained under 20 mm (climatological mean 60 mm). Saharan dust arrived above Hungary between 13–15 May. (Source of the presented data is the Hungarian Meteorological Service).

### 3. Results

#### 3.1. Evolution of Air Quality during the Lockdown

To assess the regional background air pollution impacted by the domestic as well as other European restrictions, the time series of NO, NO<sub>2</sub>, O<sub>3</sub>, and PM<sub>10</sub> pollutants are first presented at three rural sites near the country border (Figure 3). NO<sub>2</sub> levels were lower than usual; however, an important observation is that this anomaly had also been present for weeks pre-lockdown. Unusually warm late-winter induced clean air in terms of both NO<sub>2</sub> and PM<sub>10</sub>, while, accordingly, late-winter ozone concentrations were among the highest in recent years. In the first weeks of the lockdown, NO<sub>2</sub> background slightly declined, while ozone and especially PM<sub>10</sub> concentrations rose. The PM<sub>10</sub> concentration time series are extraordinary such that concentrations in April (during the curfew) were higher than in the heating season February, an extreme behavior caused by the unusually warm and dry period during these months. Peaks of a Central Asian dust transport event, coinciding with the onset of the curfew period, were also identifiable in the PM<sub>10</sub> time series. In the gradual reopening phase of May, PM<sub>10</sub> background concentrations reduced to (but not below) the multi-year range, while NO<sub>2</sub> and O<sub>3</sub> levels remained lower and higher than usual, respectively. Unique photochemical behavior was found at station #41 (Sarród), marked by elevated NO levels and corresponding low ozone concentrations. This site, although defined as a background station located in a natural environment, might have been affected by the plume of the city of Vienna (Austria), located 75 km to the northwest. High ozone concentrations can be partly attributed to the lack of NO titration at site #23 and in May at site #45. However, site #45 experienced higher than usual concentrations of both NO and O<sub>3</sub> during the curfew indicating high photochemical activity. While this can be explained by the extremely dry and sunny weather in April, the different NO responses among rural sites underline the heterogeneous photochemical response. The inverse response of PM<sub>10</sub> levels to the lockdown was clearly weather-driven. Both background O<sub>3</sub> and PM<sub>10</sub> levels were higher during the lockdown than before and after, while NO<sub>2</sub> maintained its low late-winter background without any major response on restrictions.

The urban impact of traffic reduction is demonstrated through the example of Pécs, a town of 145,000 inhabitants in Southern Hungary with three air quality monitoring sites (Figure 4, sites #34–36 in Figure 2). The sharp decline of NO<sub>x</sub> concentrations at the onset of the public emergency marks the air mass change caused by a cold front, but a gradual degradation of NO<sub>2</sub> concentrations was observable during the curfew. Comparison of sites #34–36 provides insight into urban photochemistry. The roadside location (#34) experienced a major reduction of NO levels at the onset of the restrictions, coupled with the corresponding increase in ozone concentrations. Meanwhile, at the urban background site (#36), both NO<sub>2</sub> and ozone levels were lower than usual, with a relatively high NO/NO<sub>2</sub> ratio. The magnitude of inverse chemical response of ozone was not uniform: O<sub>3</sub> concentrations during the curfew were high in the city center as well as in the suburbs, while the urban background ozone level was lower than usual. The urban NO<sub>x</sub>–O<sub>3</sub> time series was clearly different from the rural values, reflecting changes in local emissions, but the behavior of PM<sub>10</sub> mirrored the background (Figures 2 and 3). The eastern dust transport in the first days of the curfew was especially strong in this southern area of the country, causing nonattainment of the 50 µg/m<sup>3</sup> EEA guideline coinciding with the annual minimum of traffic density.

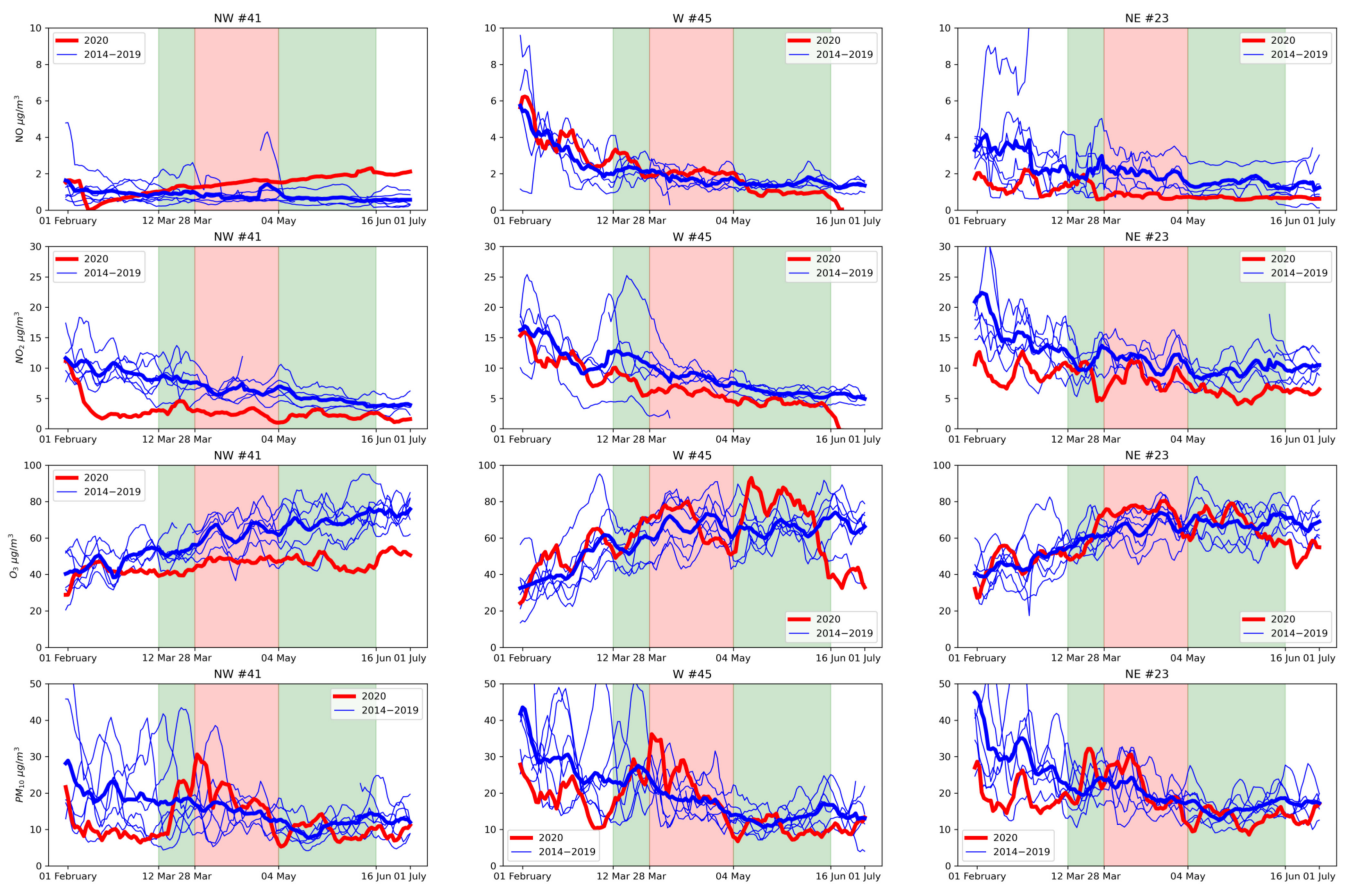


**Figure 3.** Seven-day rolling mean air pollutant concentrations in February–June 2020 (red) compared to the same periods of 2014–2019 (each year with thin blue lines; mean with thick blue line) at three rural monitoring sites near the borders of Hungary (sites #41, #45, and #23 in Figure 2). The public emergency period (green) and the curfew period (red) are marked with shaded columns.

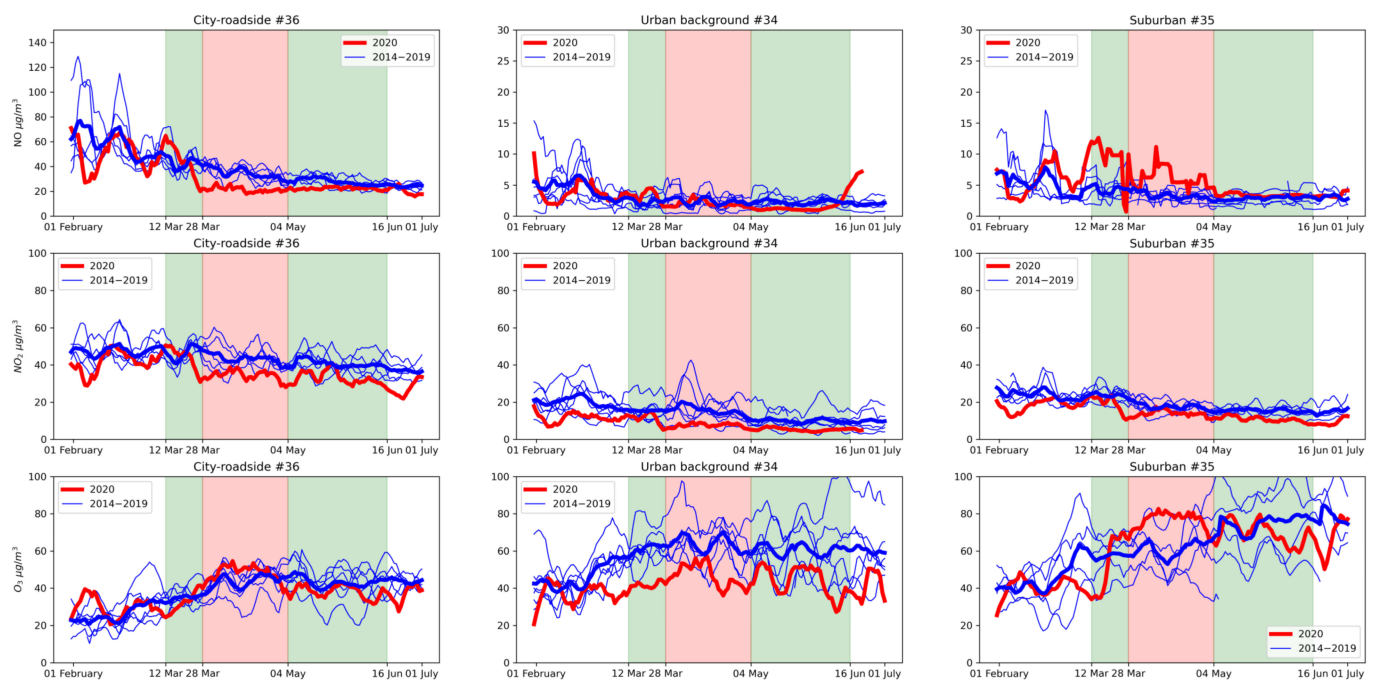


**Figure 4.** Cont.

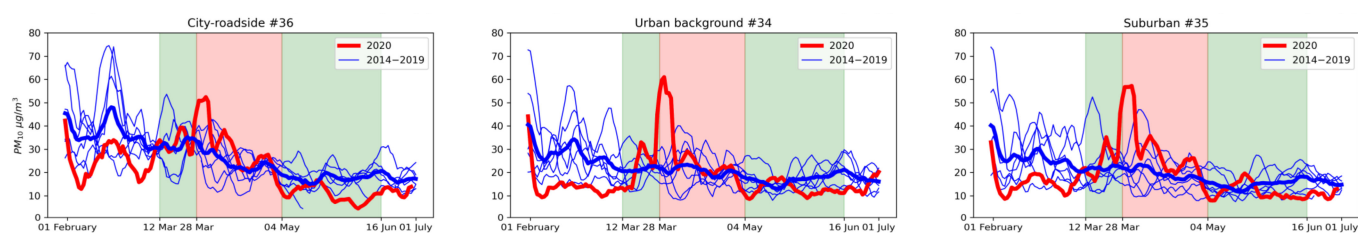


**Figure 4.** Daily mean air pollutant concentrations in February–June 2020 (red) compared to the same periods of 2014–2019 (blue) at three monitoring sites within the town of Pécs in Southern Hungary, 145,000 inhabitants (sites #34–36 in Figure 2). Note the different scale for NO at the roadside location for better visibility. The public emergency period (green) and the curfew period (red) are marked with shaded columns.

### 3.2. Comparison of Nitrogen Oxide and Ozone Levels to the Reference Years

The comparison of nitrogen oxide (NO<sub>x</sub>) and ozone (O<sub>3</sub>) concentrations of 2020 compared to the same period in 2014–2019 at all available locations are shown in Figures 5 and 6 and in Appendices B and C. At towns with multiple monitoring sites, urban/suburban responses could be distinguished. Roadside NO<sub>x</sub> concentration reductions between 21–33% or 1.6–4.1 SD in the curfew period were observed at roadside city locations (#14, #28, #22, #36, Figure 4), coupled with the decrease in NO/NO<sub>2</sub> ratio and increasing ozone concentrations. This shows that the primary impact of traffic reductions was similar among the four towns. However, the response of urban/suburban background pollution was far from being uniform. Among suburban sites, there were examples of significantly decreasing (#29, #36), increasing (#16, #35), and stagnant (#21) ozone concentrations, while corresponding suburban NO<sub>x</sub> changes ranged between −45% and +3%. This highlights the different regional chemical responses to traffic reduction. Other cities in Hungary with a single monitoring site have also shown different characteristics: significant NO<sub>x</sub> reduction with a corresponding increase in ozone concentration, significant NO<sub>x</sub> reduction with no increase in ozone levels, and no NO<sub>x</sub> reduction. NO/NO<sub>2</sub> ratio generally increased or stagnated throughout the country, except for roadside and a few urban stations.

In the capital city, Budapest, with 1.7 million inhabitants and dense traffic, the roadside city location (#12) experienced a 44% = 2.5 SD reduction of NO<sub>x</sub> concentrations during the curfew period with nearly stagnant ozone levels. Other urban and suburban background sites showed a 0–18% decrease in NO<sub>x</sub> pollution. Meanwhile, a considerable (4–63%) increase in urban/suburban background ozone pollution was experienced as a coupled effect of traffic reduction and weather. As expected, the amplitude of the response in both directions was much higher in Budapest than in the rest of the country: the temporal mean, spatial median NO<sub>x</sub> concentration in the curfew period decreased from 37 to 30 µg/m<sup>3</sup> (−28%) at locations in Budapest, while only from 22 to 21 µg/m<sup>3</sup> (−7%) in the rest of the country, compared to the 2014–2019 reference years. Meanwhile, spatial median ozone concentration increased from 50 to 64 µg/m<sup>3</sup> in Budapest (+24%), but only from 61 to 67 µg/m<sup>3</sup> (+8%) in the rest of the country.

In conclusion, the NO<sub>x</sub>–O<sub>3</sub> response to traffic reduction seems to be strongly region-specific. Ozone reduction was mostly achieved in Western Hungary despite the positive weather influence, while most of the country and most notably the capital city Budapest experienced unusually high ozone levels during the curfew with large regional and intra-urban variability.

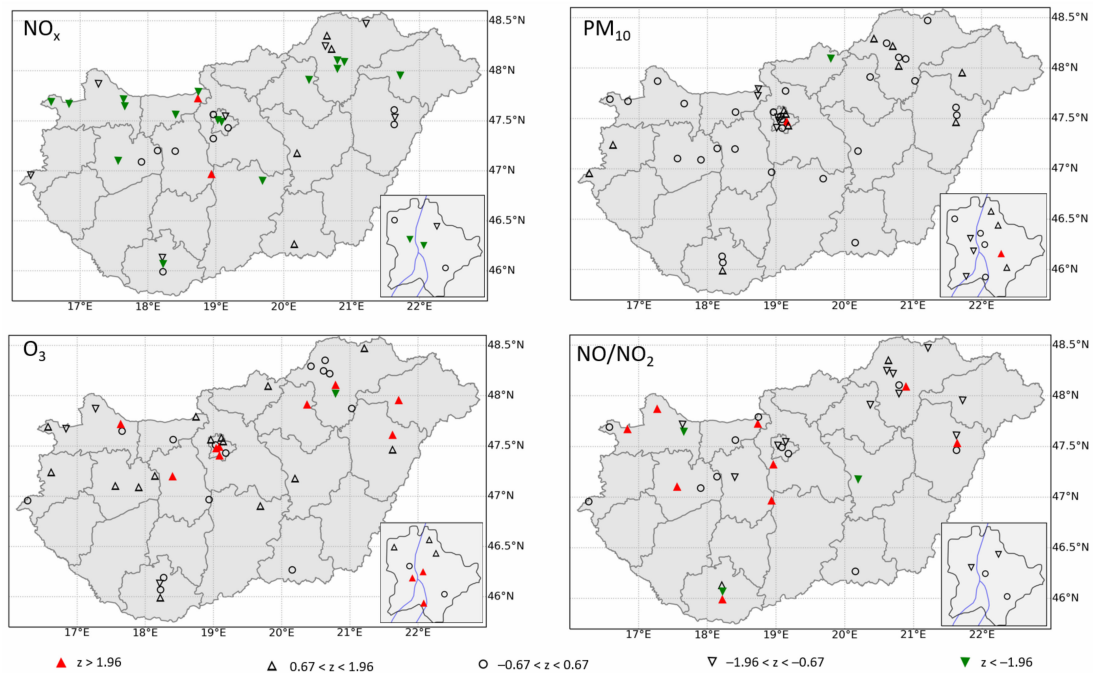


**Figure 5.** Difference of mean air pollutant concentrations and NO/NO<sub>2</sub> concentration ratio in the curfew period (28 March–4 May) in 2020 relative to the same period in 2014–2019. Green/red triangles show a significant decrease/increase (concentrations of 2020 deviating from the mean of 2014–2019 with at least 1.96 SD). Black triangles show changes between 0.67–1.96 SD. Circles show changes of any direction less than 0.67 SD. Only monitoring sites with at least 4 years with >75% daily data availability in 2014–2019 and >75% daily data availability in 2020 are marked. (Note that some markers were shifted with max. 10 km to avoid overlapping).

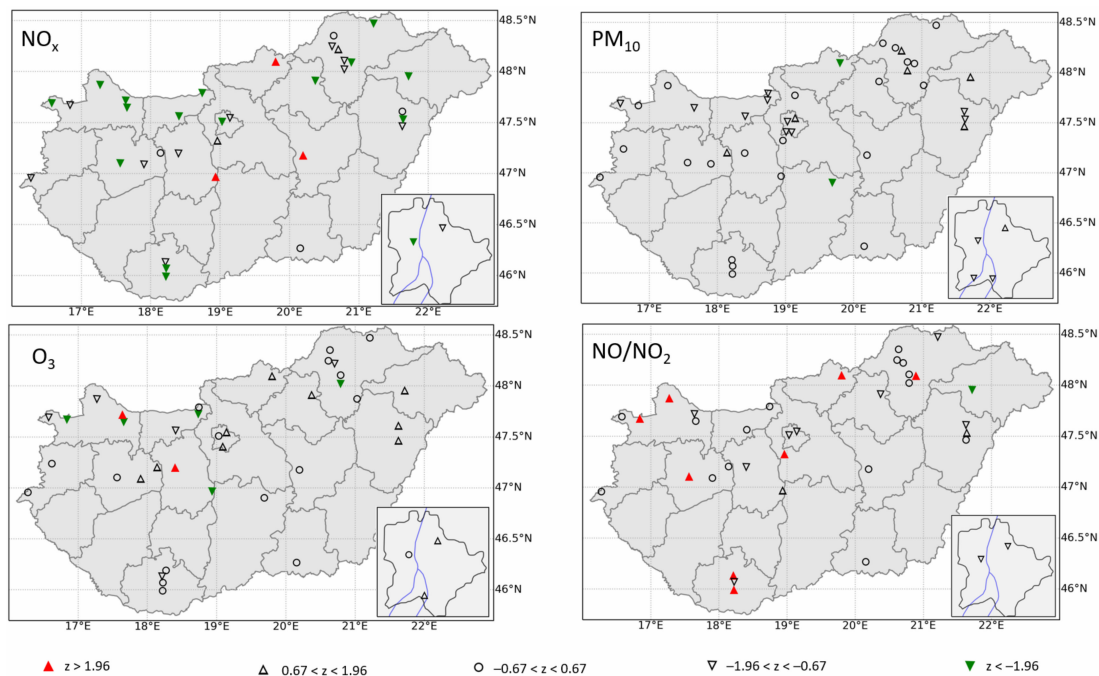


**Figure 6.** Difference of mean air pollutant concentrations and NO/NO<sub>2</sub> concentration ratio in the public emergency period (12 March–16 June) in 2020 relative to the same period in 2014–2019. Green/red triangles show a significant decrease/increase (concentrations of 2020 deviating from the mean of 2014–2019 with at least 1.96 SD). Black triangles show changes between 0.67–1.96 SD. Circles show changes of any direction less than 0.67 SD. Only monitoring sites with at least 4 years with >75% daily data availability in 2014–2019 and >75% daily data availability in 2020 are marked. (Note that some markers were shifted with max. 10 km to avoid overlapping).

### 3.3. Comparison of Particulate Matter Pollution to the Reference Years

As a superposition of emission and weather anomalies, the COVID-PM<sub>10</sub> response was modest and very heterogeneous. The comparison of PM<sub>10</sub> concentrations of 2020 compared to the same period in 2014–2019 are shown in Figures 5 and 6, and in Appendix D. In general, the spatial variability of PM<sub>10</sub> is lower, but the inter-annual variability is higher than those of gaseous pollutants, and the overall source contribution of traffic is low. Thus, the spatial structure of the response is more relevant, and no considerable difference of PM<sub>10</sub> concentrations from the reference period 2014–2019 was found. It must be noted, however, that no significant difference from previous years means increasing concentrations compared to the pre-lockdown period because of the unusually clean pre-lockdown weeks presented in Section 3.1.

The capital city, Budapest, had 11 monitoring sites available for PM<sub>10</sub> comparison. Two roadside sites (#10 and #12) gained a PM<sub>10</sub> concentration reduction of 21% and 12%, respectively. Although these values differ with only 0.7 SD from the reference mean, such reduction is unseen at most locations throughout the country and also at roadside monitoring sites in smaller towns. Suburban monitoring sites in Budapest showed a wide range of PM<sub>10</sub> responses between −18%–+28% or −0.9–+1.7 SD in the curfew period, showing that intra-urban variability of particulate pollution was large. However, it is spectacular that of the 11 monitoring sites in Budapest, six had lower PM<sub>10</sub> concentrations in the curfew period than the mean of the same period in 2014–2019. In the rest of the country, only 8 of 34 locations had reduced PM<sub>10</sub> pollution. On the other hand, the temporal mean, spatial median PM<sub>10</sub> concentration among monitoring sites within Budapest was 24 µg/m<sup>3</sup> in 2014–2019 and 29 µg/m<sup>3</sup> in 2020. For the rest of the country, the spatial median of 22 µg/m<sup>3</sup> in the reference period increased to only 23 µg/m<sup>3</sup> in 2020. The overall conclusion is ambiguous: in terms of PM<sub>10</sub> pollution, the capital city, Budapest was the only location where traffic reduction could dominate over adverse weather to reduce PM<sub>10</sub> pollution at some (roadside) sites; however, the whole of Budapest became more polluted relative to smaller towns than in usual years.

## 4. Discussion and Conclusions

In the first half of 2020, two parallel extremes affected Hungarian air quality: a weather extreme manifesting in an unusually warm late winter and a spring drought, and an emission extreme caused by the COVID pandemic.

The general response to these acting factors in the spring of 2020 was a reduction of NO<sub>x</sub> concentrations beginning weeks before the lockdown and reaching an amplitude comparable to the decrease in traffic during the pandemic. A median reduction of 16% was experienced for monitoring sites in Budapest and 21% for the rest of the country during the curfew, compared to the same period in previous years. The maximum roadside reduction in the city of Budapest reached 44% in the curfew period, which fits well within the 32–50% range obtained for U.K. roadsides [18], although it lags behind the reductions of 50–65% in the Mediterranean [3,4]. Ozone concentrations were anomalously high because of both weather and chemical reasons. A median increase of 24% in Budapest and 8% in the rest of the country was found during the curfew, compared to previous years. Similarly, a 20% increase was found in the U.K. [18] and 2–27% in the Mediterranean [4]. It must be noted, however, that obtained air pollution reductions should not be strictly compared to other reports without accounting for weather impacts and different methodology [33].

PM<sub>10</sub> concentrations were mainly weather-driven, with a strong negative anomaly in the pre-lockdown period, followed by a sharp increase at the onset of the pandemic. Although the moderation of this increase might be attributable to the traffic reduction at a few roadside locations, no overall pandemic-related changes in PM<sub>10</sub> concentrations could be demonstrated. The lack of considerable reduction in particulate concentrations was reported from the U.K. [18] and generally from Europe [21]. The latter study suspected heating and agricultural emissions behind this finding. Rodríguez-Urregos have already noticed that Budapest, as well as nearby capitals Bratislava, Vienna, and Prague, had

surprisingly increasing PM<sub>2.5</sub> concentrations during the lockdown due to an unknown reason [8]. The reason can be identified in the drought affecting this region during the curfew, as well as the unusually clean pre-lockdown period used as a reference for their comparison. Large-scale transport events also occurred, most notably the major dust transport episode on 23–27 March 2020 [32], causing poor air quality throughout the Balkans and Southern Hungary. Shen et al. provided a similar example from China for a dominant dust transport event coinciding with the lockdown [15]. Our findings confirm the results of a previous study [10] on COVID-related air quality changes in the city of Budapest, reporting a 22–39% reduction of roadside NO<sub>2</sub>, 11–80% increase in ozone levels and no considerable change in particulate concentrations.

Recognizing the serious weather dependence of short-term changes in air quality, Gkatzelis et al. highlighted the importance of weather correction when estimating COVID-AQ response to obtain comparable results among different locations and periods [33]. Meanwhile, they found that the majority of reviewed research did not apply a quantitative correction for meteorology due to limitations of available data and models, while others applied a wide variety of methods [33], including a range of statistical [22] and dynamical [21] models. Reliable statistical weather correction in the Hungarian case is challenged by the extreme weather of 2020 (February was the 3rd warmest, April and May were the 4th and 14th driest since 1901 in Hungary, respectively, according to the Hungarian Meteorological Service), while available air quality model results carry considerable uncertainty [27].

In the heating season, the daily mean temperature is considered to be a good predictor of PM<sub>10</sub> levels [27,30] through its correlation with heating emissions. Furthermore, it is a good indicator of air stagnation episodes, characterized by low (winter) or high (summer) temperature anomalies. However, with the increasing role of large-scale transport [31] and seasonal agricultural emissions, the statistical relationship between meteorological variables and air quality decays toward the summer. Spearman correlations (*s*) between daily mean temperature and air pollutant concentrations are presented in Figures S1–S3 and Tables S1–S3 of Supplementary Material. The daily mean temperature was well correlated with PM<sub>10</sub> levels during the curfew period during the reference years 2014–2019 (*s* between 0.4–0.7), but this correlation nearly disappeared in 2020 (Figure S3). This shows that while the curfew period is normally considered to be within the heating season, the unusually warm spring of 2020 eliminated the importance of heating emissions. The emergency period, including the warm months of May and part of June, showed a weak correlation with temperature. The positive correlation of ozone concentration with temperature was stronger in the emergency period, including early summer months (Figure S2). Meanwhile, in the curfew period, the correlation between temperature and ozone was much stronger in 2020 than in previous years, indicating the weather forcing behind elevated ozone levels.

A recent study found no significant trend of air pollutant gases in Budapest during the last decade, while particulate pollution declined 4–5%/year [34]. Thus, no long-term trend can be identified behind the changes that occurred in 2020. For reference, linear trends fitted on the mean concentration of the curfew period during 2014–2019 are presented in Appendices B–D for each location; however, these trends are based on only 6 years of data; thus, they are highly uncertain and barely significant.

An important notice for future studies is that the extreme weather in February 2020 with normal emissions (pre-lockdown) caused a more spectacular air quality improvement than the subsequent emission reduction with adverse weather. In fact, the half-year (January–June 2020) mean PM<sub>10</sub> pollution in Hungary was significantly lower in 2020 than in the previous years at most locations, but this was entirely attributable to the pre-lockdown winter period, while elevated PM<sub>10</sub> levels occurred during the curfew. Furthermore, the observed negative NO<sub>x</sub> anomaly had also been present for weeks pre-lockdown. In future studies, it will be necessary to consider the anomalously clean pre-lockdown winter when using it as a reference period or to calculate annual means to assess the air quality impact of the pandemic.

**Supplementary Materials:** The following are available online at <https://www.mdpi.com/article/10.3390/atmos12050561/s1>, Figure S1: Spearman correlation between daily mean temperature and NO<sub>x</sub> concentrations at selected monitoring sites, Figure S2: Spearman correlation between daily mean temperature and O<sub>3</sub> concentrations at selected monitoring sites, Figure S3: Spearman correlation between daily mean temperature and PM<sub>10</sub> concentrations at selected monitoring sites, Table S1: Spearman correlations and corresponding *p*-values between daily mean temperature and NO<sub>x</sub> concentrations at selected monitoring sites, Table S2: Spearman correlations and corresponding *p*-values between daily mean temperature and O<sub>3</sub> concentrations at selected monitoring sites, Table S3: Spearman correlations and corresponding *p*-values between daily mean temperature and PM<sub>10</sub> concentrations at selected monitoring sites.

**Author Contributions:** Conceptualization, A.V.-B., Á.L. and R.M.; methodology, A.V.-B. and Á.L.; software, A.V.-B.; investigation, Á.L.; resources, A.V.-B., Á.L. and R.M.; data curation, A.V.-B., Á.L. and R.M.; writing—original draft preparation, Á.L.; writing—review and editing, A.V.-B., Á.L. and R.M.; visualization, A.V.-B. and Á.L.; supervision, R.M.; project administration, A.V.-B. and R.M.; funding acquisition, A.V.-B. and R.M. All authors have read and agreed to the published version of the manuscript.

**Funding:** The research reported in this paper was supported by the National Research, Development and Innovation Office of Hungary (No. K128805-128818) and the ÚNKP-19-3 New National Excellence Program of the Ministry for Innovation and Technology.

**Institutional Review Board Statement:** Not applicable.

**Informed Consent Statement:** Not applicable.

**Data Availability Statement:** The data presented in this study are available in the Appendix A.

**Acknowledgments:** Authors acknowledge the data used in this study from the Hungarian Meteorological Service (OMSZ), the Hungarian Air Quality Monitoring Network (OLM), and the Budapest Public Roads Company (Budapest Közút). The authors appreciate the information on air quality instrumentation from Viktor Dézsi.

**Conflicts of Interest:** Authors declare no conflict of interest.

## Appendix A. List of Air Quality Monitoring Sites

**Table A1.** List of air quality monitoring sites in Hungary.

ID	Location	Longitude (°E)	Latitude (°N)	Surroundings	Population of Host Municipality (Thousand People)
1	Ajka	17.56	47.10	Industrial	30
2	Budapest-Budatétény	19.01	47.41	Suburban	1756
3	Budapest-Csepel	19.09	47.40	Suburban	1756
4	Budapest-Erzsébet	19.05	47.50	City, roadside	1756
5	Budapest-Gergely	19.16	47.47	Suburban	1756
6	Budapest-Gilice	19.18	47.43	Suburban	1756
7	Budapest-Honvéd	19.07	47.52	Urban	1756
8	Budapest-Káposztásmegyer	19.11	47.58	Suburban	1756
9	Budapest-Kőrakás	19.14	47.54	Suburban	1756
10	Budapest-Kosztolányi	19.04	47.47	City, roadside	1756
11	Budapest-Pesthidegkút	18.96	47.56	Suburban	1756
12	Budapest-Széna	19.03	47.51	City, roadside	1756

Table A1. Cont.

ID	Location	Longitude (°E)	Latitude (°N)	Surroundings	Population of Host Municipality (Thousand People)
13	Budapest-Teleki	19.09	47.49	Urban	1756
14	Debrecen-Hajnal	21.64	47.53	City, roadside	203
15	Debrecen-Kalotaszeg	21.62	47.51	Urban	203
16	Debrecen-Klinika	21.63	47.56	Suburban	203
17	Dorog	18.74	47.72	Industrial	12
18	Dunaújváros	18.94	46.97	Industrial	45
19	Eger	20.37	47.91	Urban	54
20	Esztergom	18.75	47.79	Urban	28
21	Győr-Ifúság	17.66	47.68	Urban	129
22	Győr-Szent István	17.64	47.69	City, roadside	129
23	Hernádszurdok	21.21	48.47	Background	0.2
24	Kazincbarcika	20.61	48.25	Industrial	29
25	Kecskemét	19.69	46.90	Urban	111
26	Komló	18.27	46.19	Industrial	26
27	Miskolc-Alföldi	20.81	48.09	Suburban	158
28	Miskolc-Búza	20.79	48.11	City	158
29	Miskolc-Lavotta	20.79	48.05	Suburban	158
30	Miskolc-Mobil	20.69	48.10	Urban	158
31	Mosonmagyaróvár	17.27	47.87	Urban	34
32	Nyíregyháza	21.72	47.96	Urban	118
33	Oszlár	21.03	47.87	Industrial	0.4
34	Pécs-Boszorkány	18.21	46.08	Urban	145
35	Pécs-Nevelési	18.22	46.04	Suburban	145
36	Pécs-Szabadság	18.23	46.07	City, roadside	145
37	Putnok	20.43	48.29	Industrial	7
38	Rudabánya	20.64	48.35	Industrial	3
39	Sajószentpéter	20.70	48.22	Industrial	12
40	Salgótarján	19.80	48.09	Industrial	35
41	Sarród	16.84	47.67	Background	1
42	Sopron	16.58	47.69	Urban	62
43	Szeged	20.15	46.27	Urban	162
44	Székesfehérvár	18.40	47.20	Urban	101
45	Szentgotthárd	16.27	46.96	Background	9
46	Szolnok	20.20	47.18	Urban	71
47	Szombathely	16.62	47.24	Urban	78
48	Tatabánya	18.41	47.56	Industrial	66
49	Tököl	18.96	47.32	Suburban	9
50	Vác	19.14	47.77	Urban	33
51	Várpalota	18.14	47.20	Industrial	21
52	Veszprém	17.91	47.10	Urban	60

## Appendix B. NO<sub>x</sub> Concentrations in the Curfew Period (28 March–4 May)

Row colors: (light) red—z-score at least +1.96 (+0.67) and the difference to the reference mean is more than 3 year’s linear trend. (light) green—z-score less than −1.96 (−0.67), and the difference to the reference mean is more than 3 year’s linear trend. Gray: absolute value of z-score less than 0.67 OR the difference to the reference mean is less than 3 year’s linear trend.

**Table A2.** Descriptive statistics and changes of NO<sub>x</sub> concentrations measured at Hungarian monitoring sites. Row colors: (light) red—z-score at least +1.96 (+0.67) and the difference to the reference mean is more than 3 year’s linear trend. (light) green—z-score less than −1.96 (−0.67), and the difference to the reference mean is more than 3 year’s linear trend. Gray: absolute value of z-score less than 0.67 OR the difference to the reference mean is less than 3 year’s linear trend.

ID	Name	Surroundings	Available Years	Mean ± SD [μg/m <sup>3</sup> ]	Relative SD	2014–2019		2020	
						Linear Trend [μg/m <sup>3</sup> /year, as Percentage of the Mean]	Mean [μg/m <sup>3</sup> ]	Difference to Reference Mean	z-Score
1	Ajka	Industrial	5	15 ± 1	7%	−3%	12	−18%	−2.6
6	Budapest-Gilice	Suburban	6	32 ± 5	17%	−4%	30	−5%	−0.3
9	Budapest-Kőrákás	Suburban	5	37 ± 5	12%	+6%	30	−18%	−1.4
11	Budapest-Pesth.	Suburban	4	20 ± 1	4%	−1%	20	0%	0.0
12	Budapest-Széna	City, roadside	6	90 ± 16	17%	+1%	51	−44%	−2.5
13	Budapest-Teleki	Urban	5	54 ± 4	6%	+1%	46	−16%	−2.5
14	Debrecen-Hajnal	City, roadside	5	66 ± 9	14%	+4%	51	−22%	−1.6
15	Debrecen-Kalota.	Urban	6	26 ± 4	13%	+1%	24	−7%	−0.5
16	Debrecen-Klinika	Suburban	6	24 ± 4	18%	−7%	24	0%	0.0
17	Dorog	Industrial	4	22 ± 7	33%	−16%	42	+89%	+2.7
18	Dunaújváros	Industrial	5	22 ± 4	17%	+5%	36	+64%	+3.7
19	Eger	Urban	6	22 ± 3	12%	−1%	16	−27%	−2.3
20	Esztergom	Urban	5	14 ± 1	8%	0%	11	−18%	−2.1
21	Győr-Ifúság	Urban	6	38 ± 5	13%	−4%	23	−39%	−3.1
22	Győr-Szentlíván	City, roadside	5	48 ± 4	8%	+1%	32	−33%	−4.1
23	Hernádszurdok	Background	4	14 ± 2	18%	−2%	9	−32%	−1.8
24	Kazincbarcika	Industrial	6	16 ± 2	10%	+5%	14	−13%	−1.2
25	Kecskemét	Urban	4	21 ± 3	12%	+4%	15	−31%	−2.5
27	Miskolc-Alföldi	Suburban	6	23 ± 2	10%	+3%	15	−34%	−3.5
28	Miskolc-Búza	City	6	66 ± 7	10%	+2%	52	−21%	−2.0
29	Miskolc-Lavotta	Suburban	4	19 ± 2	8%	−2%	14	−25%	−3.1
31	Mosonmagyaróvár	Urban	5	19 ± 3	14%	−8%	14	−26%	−1.9
32	Nyíregyháza	Urban	6	38 ± 5	12%	0%	27	−30%	−2.4
34	Pécs-Boszorkány	Urban	6	19 ± 6	33%	+10%	10	−45%	−1.4
35	Pécs-Nevelési	Suburban	6	22 ± 2	7%	+2%	23	+3%	+0.5
36	Pécs-Szabadság	City, roadside	5	95 ± 9	9%	+5%	66	−30%	−3.3
38	Rudabánya	Industrial	5	7 ± 1	16%	+5%	9	+16%	+1.0
39	Sajószentpéter	Industrial	6	15 ± 1	7%	+2%	16	+5%	+0.7
41	Sárród	Background	4	7 ± 1	15%	−2%	5	−36%	−2.4
42	Sopron	Urban	6	18 ± 2	13%	+1%	13	−27%	−2.1
43	Szeged	Urban	6	19 ± 3	17%	−7%	24	+25%	+1.5
44	Székesfehérvár	Urban	5	37 ± 16	43%	+5%	27	−29%	−0.7
45	Szentgotthárd	Background	6	12 ± 2	16%	−4%	9	−23%	−1.5
46	Szolnok	Urban	5	35 ± 7	19%	−5%	46	+32%	+1.6
48	Tatabánya	Industrial	5	24 ± 2	9%	−4%	20	−19%	−2.0
49	Tököl	Suburban	4	20 ± 3	14%	+6%	21	+2%	+0.2
51	Várpalota	Industrial	5	32 ± 10	32%	+1%	30	−5%	−0.2
52	Veszprém	Urban	5	25 ± 3	13%	+7%	24	−6%	−0.5

Appendix C. O<sub>3</sub> Concentrations in the Curfew Period (28 March–4 May)

**Table A3.** Descriptive statistics and changes of O<sub>3</sub> concentrations measured at Hungarian monitoring sites. Row colors: (light) red—z-score at least +1.96 (+0.67) and the difference to the reference mean is more than 3 year’s linear trend. (light) green—z-score less than −1.96 (−0.67), and the difference to the reference mean is more than 3 year’s linear trend. Gray: absolute value of z-score less than 0.67 OR the difference to the reference mean is less than 3 year’s linear trend.

ID	Name	Surroundings	Available Years	2014–2019			2020		
				Mean ± SD [μg/m <sup>3</sup> ]	Relative SD	Linear Trend [μg/m <sup>3</sup> /year, as Percentage of the Mean]	Mean [μg/m <sup>3</sup> ]	Difference to Reference Mean	z-Score
1	Ajka	Industrial	6	70 ± 15	21%	+8%	82	+16%	+0.7
3	Budapest-Csepel	Suburban	5	40 ± 7	18%	−9%	67	+65%	+3.6
6	Budapest-Gilice	Suburban	6	55 ± 7	14%	−1%	57	+4%	+0.3
8	Budapest-Kápm.	Suburban	5	52 ± 11	21%	+3%	70	+36%	+1.7
9	Budapest-Kórákás	Suburban	6	49 ± 9	19%	−2%	61	+25%	+1.3
10	Budapest-Koszt.	City, roadside	5	40 ± 9	23%	−1%	61	+53%	+2.3
11	Budapest-Pesth.	Suburban	6	65 ± 5	7%	+3%	72	+12%	+1.6
12	Budapest-Széna	City, roadside	6	34 ± 5	14%	+4%	33	−4%	−0.3
13	Budapest-Teleki	Urban	6	56 ± 4	8%	+2%	68	+22%	+2.8
15	Debrecen-Kalota.	Urban	6	63 ± 3	5%	+1%	67	+6%	+1.3
16	Debrecen-Klinika	Suburban	5	64 ± 5	8%	0%	75	+17%	+2.0
18	Dunaujváros	Industrial	6	49 ± 4	8%	2%	47	−5%	−0.6
19	Eger	Urban	6	60 ± 4	7%	+3%	73	+21%	+3.0
20	Esztergom	Urban	6	61 ± 7	12%	−3%	71	+17%	+1.4
21	Győr-Ifúság	Urban	6	60 ± 4	7%	+1%	59	−2%	−0.2
22	Győr-SzentIstván	City, roadside	6	51 ± 5	11%	+4%	63	+23%	+2.1
23	Hernádszurdok	Background	6	67 ± 6	9%	+4%	73	+10%	+1.1
24	Kazincbarcika	Industrial	6	60 ± 5	8%	+3%	63	+5%	+0.6
25	Kecskemét	Urban	4	72 ± 9	12%	+8%	85	+18%	+1.5
26	Komló	Industrial	4	40 ± 14	36%	+5%	43	+8%	+0.2
28	Miskolc-Búza	City	6	49 ± 2	4%	+1%	55	+12%	+2.8
29	Miskolc-Lavotta	Suburban	6	66 ± 2	3%	−1%	57	−14%	−4.2
31	Mosonmagyaróvár	Urban	5	76 ± 9	11%	+5%	69	−9%	−0.8
32	Nyíregyháza	Urban	6	58 ± 6	10%	+3%	71	+23%	+2.3
33	Oszlár	Industrial	6	61 ± 8	12%	+3%	62	+1%	+0.1
34	Pécs-Boszorkány	Urban	6	63 ± 8	14%	−6%	47	−26%	−1.9
35	Pécs-Nevelési	Suburban	5	62 ± 13	20%	+8%	76	+22%	+1.1
36	Pécs-Szabadság	City, roadside	6	44 ± 6	14%	−5%	47	+7%	+0.5
37	Putnok	Industrial	4	57 ± 8	14%	+3%	57	0%	0.0
38	Rudabánya	Industrial	6	61 ± 10	16%	+6%	63	+3%	+0.2
39	Sajószentpéter	Industrial	6	57 ± 5	8%	−1%	56	−3%	−0.3
40	Salgótarján	Industrial	4	64 ± 8	12%	+7%	72	+12%	+1.0
41	Sárród	Background	5	63 ± 9	14%	−4%	48	−23%	−1.7
42	Sopron	Urban	5	67 ± 3	5%	+2%	69	+4%	+0.8
43	Szeged	Urban	6	48 ± 10	21%	−10%	54	+14%	+0.7
44	Székesfehérvár	Urban	5	40 ± 16	40%	+11%	73	+82%	+2.1
45	Szentgotthárd	Background	6	67 ± 11	16%	+3%	67	0%	0.0
46	Szolnok	Urban	6	63 ± 13	20%	+8%	73	+15%	+0.7
47	Szombathely	Urban	6	58 ± 16	27%	+10%	69	+20%	+0.7
48	Tatabánya	Industrial	6	59 ± 4	6%	+1%	60	+2%	+0.3
51	Várpalota	Industrial	6	48 ± 17	36%	+2%	75	+57%	+1.6
52	Veszprém	Urban	6	71 ± 6	8%	+3%	77	+8%	+1.0

### Appendix D. PM<sub>10</sub> Concentrations in the Curfew Period (28 March–4 May)

**Table A4.** Descriptive statistics and changes of PM<sub>10</sub> concentrations measured at Hungarian monitoring sites. Row colors: (light) red—z-score at least +1.96 (+0.67) and the difference to the reference mean is more than 3 year’s linear trend. (light) green—z-score less than −1.96 (−0.67), and the difference to the reference mean is more than 3 year’s linear trend. Gray: absolute value of z-score less than 0.67 OR the difference to the reference mean is less than 3 year’s linear trend.

ID	Name	Surroundings	Available Years	Mean ± SD [µg/m <sup>3</sup> ]	Relative SD	2014–2019	2020		
						Linear Trend [µg/m <sup>3</sup> /year, as Percentage of the Mean]	Mean [µg/m <sup>3</sup> ]	Difference to Reference Mean	z-Score
1	Ajka	Industrial	6	20 ± 4	19%	−6%	20	0%	0.0
2	Budapest-Budatét.	Suburban	6	20 ± 4	19%	−2%	16	−18%	−0.9
3	Budapest-Csepel	Suburban	6	25 ± 6	26%	+5%	21	−17%	−0.7
5	Budapest-Gergely	Suburban	5	23 ± 3	12%	+4%	29	+26%	+2.2
6	Budapest-Gilice	Suburban	5	26 ± 5	20%	+4%	33	+28%	+1.4
7	Budapest-Honvéd	Urban	4	26 ± 4	17%	+2%	29	+9%	+0.6
8	Budapest-Kápm.	Suburban	4	20 ± 5	23%	+6%	26	+28%	+1.2
9	Budapest-Kőrákás	Suburban	6	24 ± 3	13%	−2%	29	+22%	+1.7
10	Budapest-Koszt.	City, roadside	6	23 ± 7	31%	+1%	18	−21%	−0.7
11	Budapest-Pesth.	Suburban	6	22 ± 6	25%	+3%	21	−6%	−0.2
12	Budapest-Széna	City, roadside	6	36 ± 6	17%	+3%	31	−12%	−0.7
13	Budapest-Teleki	Urban	5	30 ± 8	25%	+13%	29	−4%	−0.2
14	Debrecen-Hajnal	City, roadside	6	27 ± 3	9%	0%	27	−1%	−0.2
15	Debrecen-Kalota.	Urban	6	24 ± 3	12%	+4%	29	+18%	+1.6
16	Debrecen-Klinika	Suburban	5	24 ± 2	7%	+3%	24	−3%	−0.4
17	Dorog	Industrial	5	21 ± 3	17%	0%	18	−16%	−1.0
18	Dunaujváros	Industrial	6	26 ± 4	16%	+6%	28	+7%	+0.5
19	Eger	Urban	6	21 ± 3	16%	+5%	22	+6%	+0.4
20	Esztergom	Urban	6	19 ± 3	14%	−1%	17	−9%	−0.7
21	Győr-Ifúság	Urban	5	22 ± 5	22%	+13%	23	+3%	+0.2
23	Hernádszurdok	Background	6	20 ± 3	13%	+4%	20	+1%	+0.1
24	Kazincbarcika	Industrial	6	22 ± 3	15%	0%	24	+7%	+0.5
25	Kecskemét	Urban	5	24 ± 4	17%	+7%	22	−8%	−0.5
27	Miskolc-Alföldi	Suburban	4	28 ± 2	8%	+6%	29	+5%	+0.5
28	Miskolc-Búza	City	6	29 ± 6	20%	+7%	30	+2%	+0.1
29	Miskolc-Lavotta	Suburban	5	22 ± 3	13%	−3%	26	+17%	+1.3
31	Mosonmagyaróvár	Urban	6	21 ± 5	24%	−2%	20	−1%	0.0
32	Nyíregyháza	Urban	5	27 ± 4	15%	+7%	32	+20%	+1.3
33	Oszlár	Industrial	6	19 ± 3	17%	+7%	20	+6%	+0.4
34	Pécs-Boszorkány	Urban	6	20 ± 4	19%	+3%	22	+10%	+0.5
35	Pécs-Nevelési	Suburban	6	19 ± 6	30%	+1%	24	+29%	+0.9
36	Pécs-Szabadság	City, roadside	6	23 ± 4	18%	+3%	26	+12%	+0.6
37	Putnok	Industrial	4	23 ± 4	17%	+6%	26	+16%	+0.9
39	Sajószentpéter	Industrial	6	25 ± 5	21%	+4%	33	+32%	+1.5
40	Salgótarján	Industrial	5	25 ± 2	9%	−2%	17	−29%	−3.2
41	Sárród	Background	4	16 ± 4	26%	−2%	17	+8%	+0.3
42	Sopron	Urban	6	18 ± 4	21%	−2%	19	+2%	+0.1
43	Szeged	Urban	6	24 ± 4	17%	+8%	26	+11%	+0.7
44	Székesfehérvár	Urban	6	19 ± 9	45%	+22%	24	+25%	+0.5
45	Szentgotthárd	Background	5	18 ± 3	15%	+4%	21	+14%	+0.9
46	Szolnok	Urban	6	23 ± 3	15%	+6%	25	+7%	+0.5
47	Szombathely	Urban	5	18 ± 3	15%	+4%	21	+16%	+1.1
48	Tatabánya	Industrial	6	21 ± 3	14%	+2%	20	−3%	−0.2
50	Vác	Urban	6	25 ± 3	12%	+3%	26	+3%	+0.3
51	Várpalota	Industrial	5	17 ± 9	52%	+23%	22	+33%	+0.6
52	Veszprém	Urban	6	18 ± 5	30%	+15%	20	+12%	+0.4

### References

- Lian, X.; Huang, J.; Huang, R.; Liu, C.; Wang, L.; Zhang, T. Impact of City Lockdown on the Air Quality of COVID-19-Hit of Wuhan City. *Sci. Total Environ.* **2020**, *742*, 140556. [[CrossRef](#)]
- Collivignarelli, M.C.; Abbà, A.; Bertanza, G.; Pedrazzani, R.; Ricciardi, P.; Carnevale Miino, M. Lockdown for CoViD-2019 in Milan: What Are the Effects on Air Quality? *Sci. Total Environ.* **2020**, *732*, 139280. [[CrossRef](#)]
- Baldasano, J.M. COVID-19 Lockdown Effects on Air Quality by NO<sub>2</sub> in the Cities of Barcelona and Madrid (Spain). *Sci. Total Environ.* **2020**, *741*, 140353. [[CrossRef](#)] [[PubMed](#)]
- Sicard, P.; De Marco, A.; Agathokleous, E.; Feng, Z.; Xu, X.; Paoletti, E.; Rodriguez, J.J.D.; Calatayud, V. Amplified Ozone Pollution in Cities during the COVID-19 Lockdown. *Sci. Total Environ.* **2020**, *735*, 139542. [[CrossRef](#)]
- Siciliano, B.; Dantas, G.; da Silva, C.M.; Arbilla, G. Increased Ozone Levels during the COVID-19 Lockdown: Analysis for the City of Rio de Janeiro, Brazil. *Sci. Total Environ.* **2020**, *737*, 139765. [[CrossRef](#)] [[PubMed](#)]
- Adams, M.D. Air Pollution in Ontario, Canada during the COVID-19 State of Emergency. *Sci. Total Environ.* **2020**, *742*, 140516. [[CrossRef](#)] [[PubMed](#)]

7. Dantas, G.; Siciliano, B.; França, B.B.; da Silva, C.M.; Arbilla, G. The Impact of COVID-19 Partial Lockdown on the Air Quality of the City of Rio de Janeiro, Brazil. *Sci. Total Environ.* **2020**, *729*, 139085. [[CrossRef](#)] [[PubMed](#)]
8. Rodríguez-Urrego, D.; Rodríguez-Urrego, L. Air Quality during the COVID-19: PM<sub>2.5</sub> Analysis in the 50 Most Polluted Capital Cities in the World. *Environ. Pollut.* **2020**, *266*, 115042. [[CrossRef](#)]
9. Pei, Z.; Han, G.; Ma, X.; Su, H.; Gong, W. Response of Major Air Pollutants to COVID-19 Lockdowns in China. *Sci. Total Environ.* **2020**, *743*, 140879. [[CrossRef](#)]
10. Salma, I.; Vörösmarty, M.; Gyöngyösi, A.Z.; Thén, W.; Weidinger, T. What Can We Learn about Urban Air Quality with Regard to the First Outbreak of the COVID-19 Pandemic? A Case Study from Central Europe. *Atmos. Chem. Phys.* **2020**, *20*, 15725–15742. [[CrossRef](#)]
11. Lonati, G.; Riva, F. Regional Scale Impact of the COVID-19 Lockdown on Air Quality: Gaseous Pollutants in the Po Valley, Northern Italy. *Atmosphere* **2021**, *12*, 264. [[CrossRef](#)]
12. Zhu, Y.; Xie, J.; Huang, F.; Cao, L. The Mediating Effect of Air Quality on the Association between Human Mobility and COVID-19 Infection in China. *Environ. Res.* **2020**, *189*, 109911. [[CrossRef](#)]
13. Suhaimi, N.F.; Jalaludin, J.; Latif, M.T. Demystifying a Possible Relationship between COVID-19, Air Quality and Meteorological Factors: Evidence from Kuala Lumpur, Malaysia. *Aerosol Air Qual. Res.* **2020**, *20*, 1520–1529. [[CrossRef](#)]
14. Bolaño-Ortiz, T.R.; Pascual-Flores, R.M.; Puliafito, S.E.; Camargo-Cacedo, Y.; Berná-Peña, L.L.; Ruggeri, M.F.; Lopez-Noreña, A.I.; Tames, M.F.; Cereceda-Balic, F. Spread of COVID-19, Meteorological Conditions and Air Quality in the City of Buenos Aires, Argentina: Two Facets Observed during Its Pandemic Lockdown. *Atmosphere* **2020**, *11*, 1045. [[CrossRef](#)]
15. Shen, L.; Zhao, T.; Wang, H.; Liu, J.; Bai, Y.; Kong, S.; Zheng, H.; Zhu, Y.; Shu, Z. Importance of Meteorology in Air Pollution Events during the City Lockdown for COVID-19 in Hubei Province, Central China. *Sci. Total Environ.* **2021**, *754*, 142227. [[CrossRef](#)] [[PubMed](#)]
16. Agarwal, A.; Kaushik, A.; Kumar, S.; Mishra, R.K. Comparative Study on Air Quality Status in Indian and Chinese Cities before and during the COVID-19 Lockdown Period. *Air Qual. Atmos. Health* **2020**, *13*, 1167–1178. [[CrossRef](#)]
17. Zangari, S.; Hill, D.T.; Charette, A.T.; Mirowsky, J.E. Air Quality Changes in New York City during the COVID-19 Pandemic. *Sci. Total Environ.* **2020**, *742*, 140496. [[CrossRef](#)] [[PubMed](#)]
18. Ropkins, K.; Tate, J.E. Early Observations on the Impact of the COVID-19 Lockdown on Air Quality Trends across the UK. *Sci. Total Environ.* **2021**, *754*, 142374. [[CrossRef](#)] [[PubMed](#)]
19. Jia, C.; Fu, X.; Bartelli, D.; Smith, L. Insignificant Impact of the “Stay-At-Home” Order on Ambient Air Quality in the Memphis Metropolitan Area, U.S.A. *Atmosphere* **2020**, *11*, 630. [[CrossRef](#)]
20. Chen, L.-W.A.; Chien, L.-C.; Li, Y.; Lin, G. Nonuniform Impacts of COVID-19 Lockdown on Air Quality over the United States. *Sci. Total Environ.* **2020**, *745*, 141105. [[CrossRef](#)] [[PubMed](#)]
21. Menut, L.; Bessagnet, B.; Siour, G.; Mailler, S.; Pennel, R.; Cholakian, A. Impact of Lockdown Measures to Combat Covid-19 on Air Quality over Western Europe. *Sci. Total Environ.* **2020**, *741*, 140426. [[CrossRef](#)] [[PubMed](#)]
22. Petetin, H.; Bowdalo, D.; Soret, A.; Guevara, M.; Jorba, O.; Serradell, K.; Pérez García-Pando, C. Meteorology-Normalized Impact of the COVID-19 Lockdown upon NO<sub>2</sub> Pollution in Spain. *Atmos. Chem. Phys.* **2020**, *20*, 11119–11141. [[CrossRef](#)]
23. Velders, G.J.M.; Willers, S.M.; Wesseling, J.; van den Elshout, S.; van der Swaluw, E.; Mooibroek, D.; van Ratingen, S. Improvements in Air Quality in the Netherlands during the Corona Lockdown Based on Observations and Model Simulations. *Atmos. Environ.* **2021**, *247*, 118158. [[CrossRef](#)]
24. Grivas, G.; Athanasopoulou, E.; Kakouri, A.; Bailey, J.; Liakakou, E.; Stavroulas, I.; Kalkavouras, P.; Bougiatioti, A.; Kaskaoutis, D.G.; Ramonet, M.; et al. Integrating in Situ Measurements and City Scale Modelling to Assess the COVID-19 Lockdown Effects on Emissions and Air Quality in Athens, Greece. *Atmosphere* **2020**, *11*, 1174. [[CrossRef](#)]
25. Piccoli, A.; Agresti, V.; Balzarini, A.; Bedogni, M.; Bonanno, R.; Collino, E.; Colzi, F.; Lacavalla, M.; Lanzani, G.; Pirovano, G.; et al. Modeling the Effect of COVID-19 Lockdown on Mobility and NO<sub>2</sub> Concentration in the Lombardy Region. *Atmosphere* **2020**, *11*, 1319. [[CrossRef](#)]
26. Dong, L.; Chen, B.; Huang, Y.; Song, Z.; Yang, T. Analysis on the Characteristics of Air Pollution in China during the COVID-19 Outbreak. *Atmosphere* **2021**, *12*, 205. [[CrossRef](#)]
27. Varga-Balogh, A.; Leelőssy, Á.; Lagzi, I.; Mészáros, R. Time-Dependent Downscaling of PM<sub>2.5</sub> Predictions from CAMS Air Quality Models to Urban Monitoring Sites in Budapest. *Atmosphere* **2020**, *11*, 669. [[CrossRef](#)]
28. EEA. *Air Quality in Europe—2019 Report*; European Environment Agency: Copenhagen, Denmark, 2019.
29. Pascal, M.; Corso, M.; Chanel, O.; Declercq, C.; Badaloni, C.; Cesaroni, G.; Henschel, S.; Meister, K.; Haluza, D.; Martin-Olmedo, P.; et al. Assessing the Public Health Impacts of Urban Air Pollution in 25 European Cities: Results of the Aphekomp Project. *Sci. Total Environ.* **2013**, *449*, 390–400. [[CrossRef](#)]
30. Ferenczi, Z. Predictability Analysis of the PM<sub>2.5</sub> and PM<sub>10</sub> Concentration in Budapest. *Időjárás* **2013**, *117*, 359–375.
31. Ferenczi, Z.; Bozó, L. Effect of the Long-Range Transport on the Air Quality of Greater Budapest Area. *Int. J. Environ. Pollut.* **2017**, *62*, 407–416. [[CrossRef](#)]
32. Mahovic, N.S.; Prieto, J.; Jericevic, A.; Gasparac, G.; Smiljanic, I. Aralkum Desert Dust Pollutes Air in South-East Europe. Available online: <https://www.eumetsat.int/aralkum-desert-dust-pollutes-air-south-east-europe> (accessed on 18 April 2021).

- 
33. Gkatzelis, G.I.; Gilman, J.B.; Brown, S.S.; Eskes, H.; Gomes, A.R.; Lange, A.C.; McDonald, B.C.; Peischl, J.; Petzold, A.; Thompson, C.R.; et al. The Global Impacts of COVID-19 Lockdowns on Urban Air Pollution: A Critical Review and Recommendations. *Elem. Sci. Anth.* **2021**, *9*. [[CrossRef](#)]
  34. Mikkonen, S.; Németh, Z.; Varga, V.; Weidinger, T.; Leinonen, V.; Yli-Juuti, T.; Salma, I. Decennial Time Trends and Diurnal Patterns of Particle Number Concentrations in a Central European City between 2008 and 2018. *Atmos. Chem. Phys.* **2020**, *20*, 12247–12263. [[CrossRef](#)]